Biophysical Journal Volume 73 September 1997 1430–1439

Interaction of the Influenza Hemagglutinin Fusion Peptide with Lipid Bilayers: Area Expansion and Permeation

Marjorie L. Longo,* Alan J. Waring,# and Daniel A. Hammer*

*School of Chemical Engineering, Cornell University, Ithaca, New York 14853, and #Department of Pediatrics, Martin Luther King Jr./Drew University Medical Center and Perinatal Laboratories, Harbor-UCLA, Los Angeles, California 90059 USA

ABSTRACT Fusion is a crucial event in the infection of animal cells by enveloped viruses (e.g., HIV or influenza). Viral fusion is mediated by glycoproteins, spanning the viral envelope, which attach to a membrane surface and induce fusion of the viral envelope to the cellular membrane. Influenza fusion protein (hemagglutinin) contains an amino-terminal segment critical to fusion, referred to as the fusion peptide. We show here that the native fusion peptide (wt-20) of hemagglutinin destabilizes membranes formed of 99% 1-stearoyl-2-oleoylphosphatidylcholine (SOPC). The first step in destabilization is rapid insertion of the peptide into the membrane, in which membrane area increases by as much as 11% in just seconds. We visualized and quantified the area expansion by using optical video microscopy combined with micropipette aspiration. This rapid membrane area expansion is followed by the formation of membrane defects in the size range of 0.5 nm, and results in membrane rupture. Both the rate of area increase and maximum area increase are significantly higher at a pH near 5.0 compared to pH 7.0. These results suggest that enhanced membrane insertion of wt-20 and accompanying area expansion at pH 5.0 are responsible for the relatively greater lytic activity at this pH. We show that a deletion of the N-terminal glycine of wt-20 results in a lack of area expansion or membrane perturbation at pH 5.0.

INTRODUCTION

Membrane fusion is a critical event in the infection of all animal cells by enveloped viruses. Viral fusion is the process by which the lipid-containing membrane of the virus (envelope) and the cellular membrane become continuous, resulting in the mixing of cellular and viral aqueous compartments (White, 1992). Enveloped virus fusion reactions fall into two categories, low pH-dependent and pH-independent. Viruses with pH-dependent activity (e.g. influenza) undergo receptor-mediated endocytosis and fuse with the endosomal membrane in the low pH endosomal environment (Helenius et al., 1980; Matlin et al., 1981). pH-independent viruses (e.g., HIV) fuse mainly with the plasma membrane, but may fuse with the endosome as well (White, 1990; Grewe et al., 1990; Sinangil et al., 1988; McClure et al., 1988).

Enveloped viruses employ specific glycoproteins (viral fusion proteins) spanning the viral envelope to mediate attachment to a membrane surface and to induce fusion. For fusion to occur, these glycoproteins bridge the gap between the envelope and the cellular membrane and cause disruption and reorganization of the envelope and cellular membrane, leading to fusion. A striking feature of most viral fusion proteins is the presence of a fusion peptide. A large number of fusion peptides that have been identified are found on the amino-terminal end of the fusion protein, external to the viral envelope (Hoekstra, 1990). It has been demonstrated that the fusion peptide becomes embedded in the neighboring cellular membrane before fusion (Stegmann et al., 1991; Harter et al., 1989; Weber et al., 1994). However, very little is known of the mechanism of disruption and reorganization of the target membrane, or the dynamics of these processes.

The fusion peptides of both pH-dependent and pH-independent viruses contain a large number of apolar amino acid residues. Fusion peptides show a tendency to form "sided helices," with most of the bulkier, more hydrophobic residues found on one hemiface of the helix, and most of the smaller apolar amino acids (e.g., alanine and glycine) residing on the other side of the helix (White, 1990). Although the relevance of this helical formation to membrane fusion has been argued (Gallaher et al., 1992; Gray et al., 1996), the apparent role of segregation of hydrophobic residues is to interact with the hydrophobic chains of the membrane lipids during and before fusion.

Many viral fusion peptides have been synthesized (Steinhauer et al., 1995; Wharton et al., 1988; Düzgüneş and Shavnin, 1992; Düzgüneş and Gambale, 1988; Burger et al., 1991; Lear and DeGrado, 1987; Rafalski et al., 1991; Ishiguro et al., 1993; Slepushkin et al., 1990; Mobley et al., 1995; Glushakova et al., 1992; Wagner et al., 1992). The activity of the fusion peptide is often measured by its ability to fuse and/or lyse (cause leakage) of vesicles or red blood cell membranes (hemolysis) (Wharton et al., 1988; Wagner et al., 1992; Mobley et al., 1995; Düzgüneş and Shavnin, 1992; Lear and DeGrado, 1987; Rafalski et al., 1991). In these studies, fusion is generally accompanied by lysis and/or leakage of contents; thus the actual ability of fusion peptides alone to cause fusion has been argued. Nonethe-

Received for publication 7 October 1996 and in final form 13 June 1997.

Address reprint requests to Dr. Daniel A. Hammer, Department of Chemical Engineering, University of Pennsylvania, 392 Towne Building, 220 S. 33rd St., Philadelphia, PA 19104. Tel.: 215-573-6761; Fax: 215-573-2093; E-mail: hammer@seas.upenn.edu.

Dr. Longo's present address is Department of Chemical Engineering and Materials Science, University of California, Davis, CA 95616.

0006-3495/97/09/1430/10 $2.00

less, the lytic activity of fusion peptides correlates well with their in vivo fusion activity. For example, the lytic activity of wild-type peptides of influenza virus increases greatly as the pH decreases to ~5 (endosomal pH) (Wharton et al., 1988; Rafalski et al., 1991; Wagner et al., 1992; Düzgüneş and Shavnin, 1992). Furthermore, mutant peptides corresponding to viruses with no or reduced fusion activity do not enhance the release of solutes from vesicles (Düzgüneş and Gambale, 1988).

The pH-dependent lytic activity of certain fusion peptides makes them ideal for use in gene transfer systems (Anderson, 1995; Morsy et al., 1993) for rupture of the endosomal membrane. These gene transfer systems are much simpler, and potentially more compact, than virus-based systems that use reproductive deficient adeno- or retroviruses. Peptide-based gene transfer systems involve the formation of aggregates, containing DNA, fusion peptide, and positively charged polymer, or lipid held together by electrostatic interactions. These aggregates are internalized by endocytosis. Fusogenic peptides of influenza virus have been used successfully for rupture of the endosomal membrane, resulting in release of DNA into the cell cytoplasm (Curiel et al., 1991; Plank et al., 1994; Wagner et al., 1992).

Using micropipette aspiration, we have concentrated our efforts on measuring the interaction of fusion peptides of the well-studied influenza hemagglutinin (HA) fusion protein (from the X31 strain) with unilamellar vesicles (Soltesz and Hammer, 1995). The fusion peptide region of HA was initially identified by demonstrating that deletions in the fusion peptide region of the complete fusion protein resulted in diminished viral fusion (Daniels et al., 1985; Gething et al., 1986). The 20-amino acid fusion peptide from X31 (Wharton et al., 1988), referred to as wt-20, contains three negatively charged residues that are partially neutralized at a pH of 5, corresponding to the pH of the endosome. wt-20 becomes more α-helical at a pH of 5, in comparison to a pH of 7, when in the presence of phosphatidylcholine membranes (Wharton et al., 1988). This peptide is reported to lyse red blood cells at a pH of 5 and 7, with approximately four times greater lytic activity at pH 5 (Wharton et al., 1988). Furthermore, wt-20 shows diminished fusion activity as the pH is raised from 5 to 7 (Wharton et al., 1988).

Viral membrane fusion and membrane disruption caused by fusion peptides are dynamic processes, occurring on time scales of minutes and seconds (Stegmann et al., 1991; Hoekstra et al., 1985; Zimmerberg et al., 1994; Hug and Sleight, 1994; Lear and DeGrado, 1987; Ishiguro et al., 1993; Slepushkin et al., 1990; Glushakova et al., 1992; Struck et al., 1981; Fonteijn et al., 1992; Bagai et al., 1993; Melikyan et al., 1993; Wharton et al., 1988; Düzgüneş and Shavnin, 1992; Rafalski et al., 1991; Mobley et al., 1995). Although circular dichroism, Fourier transform infrared spectroscopy, tryptophan fluorescence, and spin labeling (for examples see Wharton et al., 1988; Clague et al., 1991; Lear and DeGrado, 1987; Rafalski et al., 1991; Gray et al., 1996) have been used to obtain information regarding bulk structural or orientational changes of fusion peptides that occur as a result of association with membrane bilayers, there is little information on the dynamics of peptide insertion into the membrane. Furthermore, there is little information on the resulting restructuring of the membrane or the formation and evolution of membrane defects.

We focus here on the use of micropipette aspiration to detect the insertion of a fusion-active peptide (wt-20) and a fusion-defective peptide (ΔG1) of HA into lipid membranes and monitor the resulting membrane instabilities. With micropipette aspiration, we can directly expose a single-membraned vesicle to a peptide-containing solution at a controlled membrane tension. Exposure can proceed under various solution conditions critical to fusion. Uptake of inserting species in the membrane can be detected by expansion of the vesicle surface area, and the formation of porous defects (Zhelev and Needham, 1993; Needham and Zhelev, 1995) can be detected directly. Micropipette aspiration uses vesicles that are sufficiently large (~25 μm in diameter) that changes in the projected area, aspirated into a micropipette, can be monitored by an optical microscope (Needham and Zhelev, 1995; Simon et al., 1994). Exposure of the vesicle to fusion peptide results in an easily detectable increase in the projected area, giving directly the change in membrane surface area due to the incorporation of fusion peptide. The formation of porous defects of a size slightly larger than that of glucose (solute outside of vesicle, diameter $\approx$ 0.5 nm; Needham and Zhelev, 1995) results in the diffusion of glucose into the vesicle and the cotransport of water. This transport causes vesicle swelling, leading to an observable decrease in the length of the projection in the pipette. In addition, changes in mechanical properties and the tensile strength of a vesicle due to peptide insertion can be measured.

MATERIALS AND METHODS

Materials

1-Stearoyl-2-oleoylphosphatidylcholine (SOPC) and 1-palmitoyl-2-oleoylphosphatidylserine (POPS) were purchased from Avanti Polar Lipids (Alabaster, AL) and were used without further purification. Chloroform and methanol used to form lipid films for vesicle production were from Fisher (Fairlawn, NJ) and were high-performance liquid chromatography (HPLC) grade. All solutes used were from Sigma (St. Louis, MO) and were ultra grade. Water was obtained from a Milli-Q UV Plus system (Millipore, Bedford, MA).

The two peptides synthesized were based on the HA fusion-active (wt-20) and fusion-defective (ΔG1) peptides previously synthesized by Wharton et al. (1988):

```
wt-20 GLFGAIAGFIENGWEGMIDG

ΔG1   LFGAIAGFIENGWEGMIDG
```

Peptides were stored frozen in dimethyl sulfoxide (DMSO) (Fisher, HPLC grade) at 1 mM concentration. Peptides were mixed with buffer solution immediately before use.

The wt-20 peptide was synthesized for us by Star Biochemicals (Torrance, CA). The molecular mass of the peptide was confirmed for us by Multiple Peptide Synthesis (San Diego, CA).

The ΔG1 peptide was synthesized on a 0.25 mmol scale with an ABI model 431A peptide synthesizer using FastMoc chemistry (Fields et al.,

1991). Peptide synthesis reagents, including solvents and Fmoc amino acid derivatives, were from Perkin-Elmer Applied Biosystems (Foster City, CA). A prederivatized Wang *p*-benzyloxybenzyl alcohol resin (Applied Biosystems) with the C-terminal glycine was used for the stepwise synthesis of the peptide. All residues were double-coupled to optimize the yield of the fusion peptide sequence. After cleavage of the peptide from the resin, the crude product was purified by reverse-phase HPLC employing a Vydac C4-column (Vydac, Hesperia, CA). The material was chromatographed by using a 60-min linear gradient, with a starting phase of water and an eluting phase of 100% acetonitrile containing 0.1% trifluoroacetic acid as an ion-pairing agent. After concentration of the peptide by vacuum centrifugation, the peptides were freeze-dried from acetonitrile:10 mM HCl (1:1, v:v) to remove any counterions from the chromatography solvent. The molecular mass of the peptide was then confirmed by fast atom bombardment mass spectroscopy (Center for Molecular and Medical Sciences Mass Spectrometry, University of California, Los Angeles, CA).

Preparation of vesicles

Vesicles containing 100 mM sucrose were formed of 99% SOPC and 1% POPS by modification of an electric field technique developed by Angelova et al., 1992. We included 1% POPS to prevent vesicle aggregation and adhesion to chamber surfaces. Briefly, 50 μl of a chloroform:methanol (2:1) solution containing 0.5 mg/ml of lipid (99% SOPC, 1% POPS) was applied to two electrodes formed of 1-mm-diameter platinum wire (Aldrich, Milwaukee, WI). A 100-μl syringe was used to spread this solution on the electrodes. After drying under mild vacuum for 2 h, the electrodes, placed 3 mm apart, were sealed in a chamber (volume of ~1.5 ml). The chamber was filled by syringe with 100 mM sucrose solution. A 3-V, 10-Hz sine wave was applied for half an hour across the two wires with a signal generator (BK Precision, Chicago, IL). Subsequently, the frequency was lowered to 3 Hz for 15 min, 1 Hz for 7 min, and 0.5 Hz for 7 min. The vesicles were harvested by flowing an additional 1.5 ml of sucrose solution through the chamber. This technique yields mainly unilamellar large vesicles, with a large percentage between 20 μm and 30 μm useful for micropipette aspiration. Vesicles were no longer used 3 days after production.

Micropipette aspiration chamber

The chamber used in these experiments (Fig. 1) contained two sections separated by a 1/32-inch-thick teflon sheet. A 0.9-mm hole was bored through the separator to allow transfer of vesicles from one section to another via micropipette. The hole remained blocked via capillary tubing until the vesicle was transferred from one side to the other. Water-saturated nitrogen was delivered to the air-solution interface of both sections to minimize evaporation.

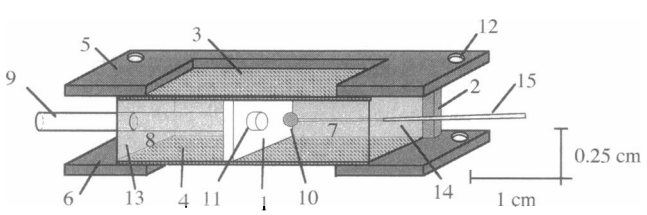

FIGURE 1 Schematic of micropipette aspiration chamber used in these experiments. The chamber is made by sandwiching a teflon spacer (*1*), four plexiglass spacers (these define the chamber size, one is visible here) (*2*), and two coverslips (*3,4*) between two aluminum plates (*5,6*) held together by screws (screw hole shown here) (*12*). The teflon spacer divides the chamber into two sections. One section (*7*) is ~200 μl in volume and contains a buffer solution with vesicles. The other section (*8*) is ~150 μl in volume and contains the buffer solution with fusion peptide. Evaporation is minimized by delivering saturated nitrogen to the air-solution interfaces (*13,14*). When a vesicle, held by the micropipette (*15*), is transferred from section 7 to section 8, the capillary tubing (*9*) remains stationary, and the entire chamber is moved from left to right by using the microscope stage. As a result, a single vesicle (*10*) is transferred through the 0.9-mm hole (*11*) and exposed to peptide solution in section 8. Only one vesicle is transferred per experiment.

Production and calibration of micropipettes

Capillary glass (Friedrich and Dimmock, Millville, NJ) was heated and elongated with a David Kopf Instruments (Tujunga, CA) micropipette puller. The glass was approximately broken at an inner diameter of 8 μm. Subsequently, a clean break was obtained with a microforge (Technical Products International, St. Louis, MO) (Needham, 1993). Micropipettes were then coated with a nonsticking agent, Surfasil (Pierce, Rockford, IL), from a 1% solution in chloroform. Pipettes used were between 7.0 μm and 9.0 μm in inner diameter.

Precise measurement of the inner diameter of each pipette was accomplished during the production of pipettes. Briefly, glass needles were drawn on the pipette puller, coated with gold, and imaged by scanning electron microscopy. Image analysis was used to obtain the length versus width profiles of the needle tips. Each profile was fitted with a fifth-order polynomial. When each pipette was produced, a glass needle was gently inserted as far as possible down the bore of the pipette. The fifth-order polynomial was used to obtain the width of the pipette from the length of insertion.

Micropipette aspiration

One half-hour before aspiration began, the 200-μl section of the chamber (see Fig. 1) was filled with a solution containing 100 mM glucose, 1 mM Na citrate, 1 mM HEPES, 1 mM 2-(*N*-morpholino)ethanesulfonic acid, and 0.03 weight% bovine serum albumin (fraction V, low heavy metals; Calbiochem-Novabiochem, La Jolla, CA), pH adjusted with 1 N and 0.1 N NaOH or HCl solutions. The 150-μl section was filled with the same solution containing peptide (which had been dispersed from a 1 mM solution in DMSO with vortexing). The maximum concentration of DMSO was 2% for a 20 μM peptide solution. Pretreating the chamber for one half-hour with the albumin present in the test solutions results in the dissipation of charges on the glass microscope slides used in the chamber (Needham, 1993). Therefore, the albumin is thought to bind strongly to the glass in the chamber. After one half-hour, ~6 μl of vesicle solution was transferred to the 200-μl chamber.

Aspiration of vesicles was performed by the use of a two-chambered manometer with attached Validyne (Northridge, CA) pressure transducers and monitor. Initially, a test vesicle was aspirated by micropipette suction to determine the area compressibility (K) and lysis tension (τ_{lyse}) (for good references on material properties measurements by micropipette aspiration, see Evans and Needham, 1987, and Evans and Rawicz, 1990). This procedure was followed to confirm that the vesicles had the same basic properties at the start of the experiments and to obtain a mean K and τ_{lyse} for normal vesicles. Area compressibility data were obtained by increasing the suction pressure on the vesicle in a stepwise manner (~4 cm water per step) until the vesicle lysed. From the suction pressure changes (ΔP), we calculated the isotropic tension τ ($\tau = \Delta P R_p/2\{1 - R_p/R_o\}$), where R_p and R_o are the pipette and exterior segment radii, respectively. From the accompanying changes in the projection length (ΔL), we calculated the areal strain, α (α can be closely approximated by $1/2\{(R_p/R_o)^2 - (R_p/R_o)^3\}\Delta L/R_p$; Evans and Rawicz, 1990). The area compressibility modulus, K, was determined by the slope of the isotropic tension, τ, versus areal strain, α. τ_{lyse} was determined as the tension of vesicle lysis.

Immediately after the compressibility and lysis tension test, a vesicle was chosen for the insertion experiment. The vesicle was prestressed to ~4 dyn/cm to ensure that the vesicle membrane was completely flattened. Subsequently, the aspiration pressure was lowered and maintained throughout the rest of the experiments to give a constant membrane tension between 0.1 and 0.2 dyn/cm. The vesicle was positioned ~150 μm from

the capillary tubing blocking the hole connecting the two sections of the chamber. The entire chamber was moved by using the microscope stage, yielding the removal of the capillary tubing from the hole and the transfer of the vesicle from the 200-μl chamber section to the 150-μl section containing the peptide. Insertion was monitored by measuring the change in projection of the vesicle in the pipette as the vesicle membrane area increased.

Area expansion, area compressibility, and lysis tension data were recorded with a Nikon inverted diaphot-TMD microscope equipped with Hoffman optics (Modulation Optics, Greenvale, NY), a Videoscope CCD-200 video camera (Washington, DC), a video encoder (suction pressure and time are encoded frame by frame on all images; courtesy of R. Waugh, University of Rochester, NY), and a SONY SVO-9500 VCR. Image analysis software and hardware (Inovisions Corporation, Durham, NC) were used to obtain vesicle dimensions, projection versus time data, and the images shown here.

RESULTS

pH-dependent insertion of wt-20

To measure the insertion of wt-20 into SOPC:POPS (99:1) vesicle bilayers at various pHs, single vesicles were transferred from a solution (containing no peptide) at the test pH to the chamber section containing 10 μM peptide (at the same pH). When we exposed a vesicle at pH 5.0 to a solution containing 10 μM wt-20, the projection increased because of membrane insertion of wt-20 (Figs. 2 *A–C* and 3 *A*). Typically, the projection increased by ~15 μm for an 8-μm pipette. Subsequently, the vesicle swelled, because of the cotransport of water and the relatively smaller sugar species, glucose, through porous defects in the membrane (Needham and Zhelev, 1995). Swelling caused the vesicle projection in the pipette to decrease (Figs. 2 *D–E* and 3 *A*). Eventually, the vesicle membrane bilayer area stretched beyond a critical area expansion, which lead to failure (lysis) of the vesicle membrane. When lysis occurred, the vesicle was slowly aspirated into the pipette bore (Fig. 2 *F*). Increases in projection (ΔL) (Figs. 2 and 3 *A*) were converted into membrane area changes, normalized by the initial area of the vesicle ($\Delta A/A_o$), plotted versus time, allowing the comparison of measurements taken from ves-

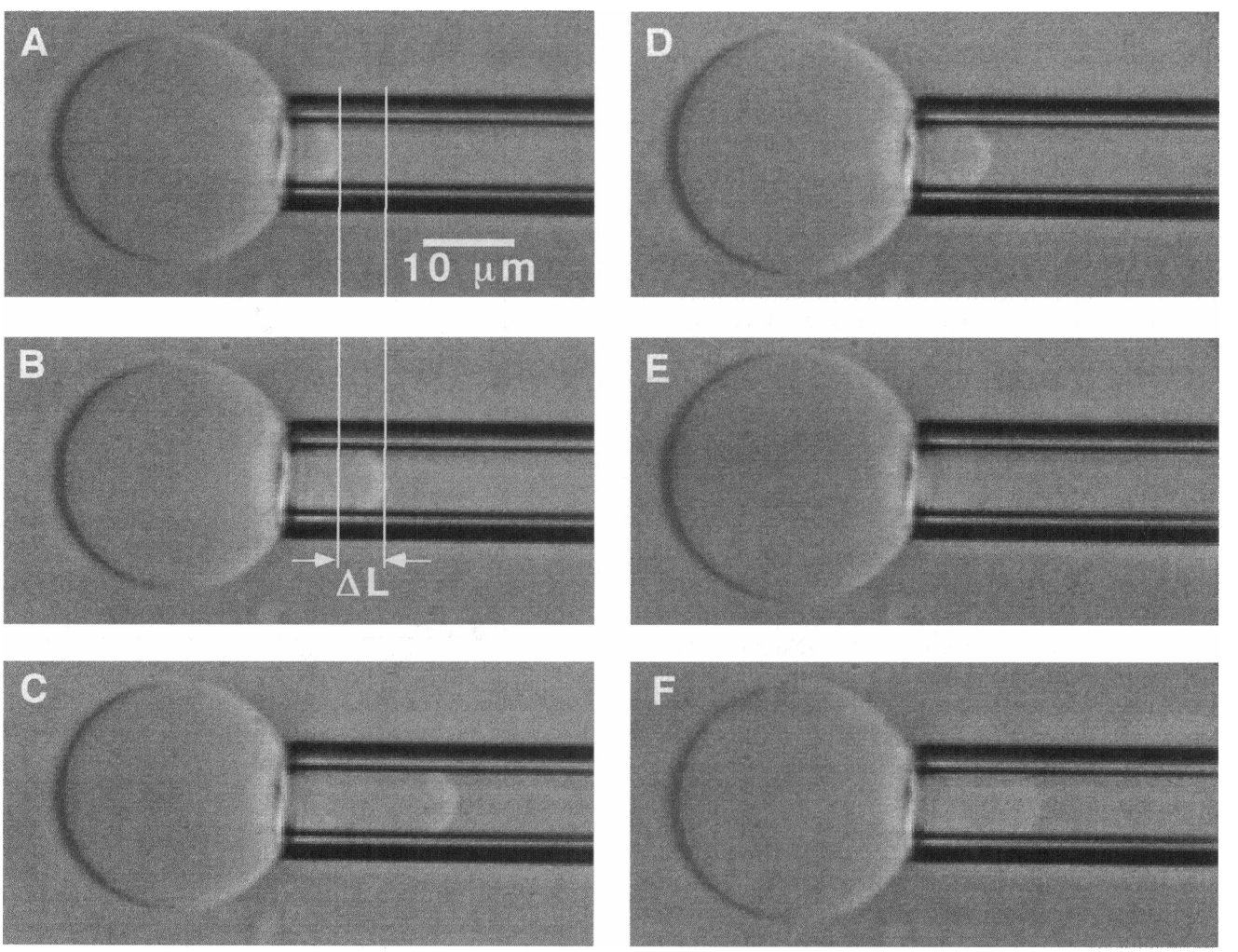

FIGURE 2 Sequential videomicrographs of a large unilamellar vesicle held under constant, low membrane tension (0.15 dyn/cm) exposed to 10 μM wt-20 at pH 5.0. (*A*) At the moment of exposure. (*B,C*) Increase in vesicle projection length (ΔL) resulting from the adsorption and intercalation of wt-20. (*D,E*) The formation of porous defects and the permeation of glucose and water into the vesicle has caused the vesicle to swell, resulting in a decreased projection length. (*F*) The vesicle lyses and is aspirated into the pipette bore because of the mild suction in the pipette.

icles and pipettes of various sizes $\Delta A = 2\pi R_p(1 - R_p/R_o)\Delta L$ (Evans and Needham, 1987). Swelling of the vesicle was monitored by the magnitude of the decrease in the projection length. These measurements were converted into volume changes normalized by the volume of the vesicle at the onset of swelling ($\Delta V/V_o$). The calculation of $\Delta V/V_o$ is based on the volume change indicated by the decrease in projection length. The total change in volume was found to be consistent with measurements taken of the vesicle volume outside of the pipette before rupture.

The area expansion profiles ($\Delta A/A_o$ versus time) of vesicles exposed to 10 μM wt-20 at pH 5 through 7.0 show the dramatic effect of pH on the vesicle area expansion resulting from the insertion of this peptide (Fig. 3 *B*). The initial rate of area expansion, the time at which the membrane became porous, and maximum area expansion were pH dependent (Table 1 and Fig. 3, *B* and *C*). Table 1 reports results for all runs performed. For each run at pH 6 and 7, a relatively small amount of area expansion was followed by a plateau. The presence of the plateau, with an almost undetectable change in area with time, may indicate that the membrane was nearing the equilibrium membrane concentration of wt-20. The plateau was followed by a decrease in the vesicle projection length, resulting from the permeation of the vesicle to glucose and water, and eventual lysis. Significant qualitative differences are shown in the area expansion plots when vesicles were exposed to wt-20 at a pH of 5.0. At a pH of 5.0, wt-20 adsorption resulted in an average maximum area fraction change, $\Delta A/A_{o,max}$, of ~0.09 (compared to $\Delta A/A_{o,max}$ of ~0.04 at a pH of 6.0). At a pH of 6.0, the permeation start times recorded were ~6 and 7 min. In comparison, the average permeation start time at pH 5.0 was ~80 s. A closer look at the area expansion plots (Fig. 3 *C*) and data (Table 1) of vesicles exposed to wt-20 at pH 4.5, 5.0, and 5.5 shows that significant increases in area expansion began at pH 5.0 (corresponding roughly to the endosomal pH).

To demonstrate that the area expansion and lysis tension observed were not simply due to the small amount of DMSO used to solubilize the peptides, we transferred vesicles to pH 5.0 and pH 7.0 solutions containing 1% DMSO, corresponding to the amount used in these experiments. We found that transfer of vesicles to 1% DMSO in buffer solution resulted in small increases in projection length relative to vesicles in wt-20 at pH 5.0. This baseline change in projection was due to a difference in osmotic strength between the two sections of the chamber and some evaporation that occurs during the experiment. Transferring a vesicle to this slightly hypertonic solution caused the vesicle volume to shrink, thus balancing the osmotic strength inside and outside of the vesicle. The projection length increased slightly to accommodate the decrease in volume. The volume decrease, normalized by the initial volume of the vesicle ($\Delta V/V_o$) versus time, is shown in Fig. 3 *B*. This change in osmotic strength was present in all experiments shown here; this apparent contribution to $\Delta A/A_o$ versus time is shown in Fig. 3 *B*. Thus the values of $\Delta A/A_{o,max}$ for all

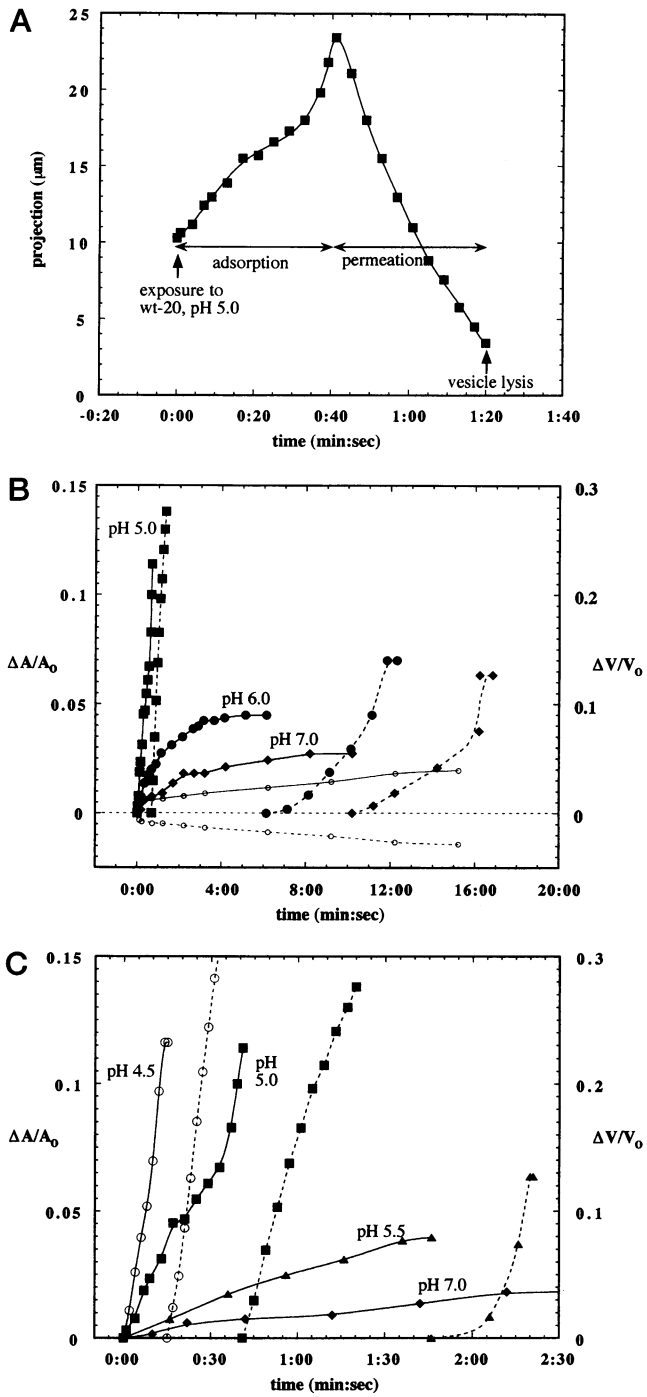

FIGURE 3 (*A*) Raw projection versus time data for exposure of vesicle to 10 μM wt-20 at pH 5.0. (*B,C*) Fractional area changes ($\Delta A/A_o$, *axis on left*) and fractional volume changes ($\Delta V/V_o$, *axis on right*) versus time for vesicles exposed to 10 μM wt-20: ◆, pH 7.0; ●, pH 6.0; ▲, pH 5.5; ■, pH 5.0; ○, pH 4.5; ○, 1% DMSO, pH 7.0. ——, $\Delta A/A_o$; – – –, $\Delta V/V_o$. Area expansion due to uptake of wt-20 occurred to a greater extent at pH 5 compared to pH 7. When vesicles are exposed to the buffer solution containing the same concentration of DMSO used to solubilize the peptide, the vesicle volume decreases slightly because of a small increase in external osmotic strength. Therefore a baseline $\Delta A/A_o$ in all experiments can be estimated by the apparent area expansion (an example run is shown here; ○).

TABLE 1 Data for exposure of vesicles to hemagglutin peptides

pH	Concentration (μM)	Permeation start time (min:s)	$\Delta A/A_{o,\,max}$* (maximum $\Delta A/A_o$ increase)
wt-20			
4.5	10	0:15	0.116
4.5	10	0:14	0.130
5.0	10	0:41	0.114
5.0	10	1:45	0.0886
5.0	10	1:25	0.0947
5.0	10	0:30	0.123
5.0	10	0:50	0.0521
5.0	10	3:15	0.0873
5.5	10	1:46	0.0396
6.0	10	7:08	0.0385
6.0	10	6:05	0.0290
7.0	10	10:12	0.0181
7.0	10	6:05	0.0255
4.5	20	0:09	0.122
4.5	5	3:20	0.114
4.5	5	1:31	0.100
4.5	5	1:16	0.0893
4.5	2.5	6:30	0.0476
4.5	1	—	0.0140
4.5	1	—	0.0170
ΔG1			
5.0	10	—	0.00678
5.0	10	—	0.00342
5.0	10	—	0.0117
7.0	10	—	0.00893
DMSO (controls)#			
pH 7.0		—	0.00653
pH 7.0		—	0.0172
pH 5.0		—	0.00624
pH 5.0		—	0.00298

Time for permeation to start after exposure to peptide and maximum fractional area increases.
*Maximum area increase (at plateau if present) divided by initial area before peptide exposure.
#No peptide, 1% DMSO.

measurements should be compared to DMSO control values (Table 1).

We compared the area compressibility (K) and lysis tension (τ_{lyse}) of vesicles exposed to DMSO with vesicles that were not exposed to DMSO and found them to be comparable. The mean K of vesicles that were not exposed to DMSO (vesicles in glucose buffer, pH 4.5–7.0) was found to be 166 dyn/cm (SD 14 dyn/cm, with all vesicles within 1.75 times the SD of the mean). The mean τ_{lyse} of vesicles (no DMSO) was found to be 7.0 dyn/cm (SD = 1.6 dyn/cm, with all vesicles within 1.75 times the SD of the mean). The K of pH 5.0 and pH 7.0 vesicles exposed to 1% DMSO was 170 dyn/cm and 154 dyn/cm, respectively. Values of τ_{lyse} for pH 5.0 and pH 7.0 vesicles exposed to 1% DMSO were 9.0 dyn/cm and 8.67 dyn/cm, respectively.

Inactive ΔG1 mutant insertion

To determine if differences in area expansion could distinguish an active fusion peptide from an inactive peptide, we monitored the area expansion of vesicles exposed to a peptide with decreased fusion and negligible hemolytic activity in comparison to wt-20 (Wharton et al., 1988). This fusion-defective peptide, referred to as ΔG1 (see Wharton et al. 1988), has an amino acid sequence identical to that of wt-20, but the N-terminal glycine is absent. We found (Fig. 4) that at both pH 5.0 and pH 7.0, exposure of vesicles to a 10 μM solution of ΔG1 resulted in a $\Delta A/A_o$ change similar to control experiments containing DMSO alone (see explanation above). The lysis tension of these vesicles was tested after ~15 min and was found to be comparable (5.97 dyn/cm at pH 5.0 and 7.22 at pH 7.0) to the lysis tension of control vesicles (reported above).

Effect of pH change on insertion

To mimic the low pH environment encountered by influenza virus in the endosome, we transferred a vesicle from a solution containing a small amount (2.5 μM) of wt-20 at a pH of 7.00 to another solution containing the same amount of wt-20 at pH 5.0 (Fig. 5). This procedure allowed us to trigger the area expansion of the vesicle, resulting from the pH-dependent change in conformation of wt-20 (Fig. 5). Retransfer to the pH 7.0 solution resulted in complete recovery of the original vesicle size, presumably because of desorption of wt-20. After desorption, the lysis tension was tested and was found to be within normal range at 5.77 dyn/cm. In a separate control experiment (data not shown), vesicles transferred to a pH 7.0 solution containing 2.5 μM wt-20 do not exhibit area expansion from the insertion of wt-20 over the time scales of this experiment. Furthermore,

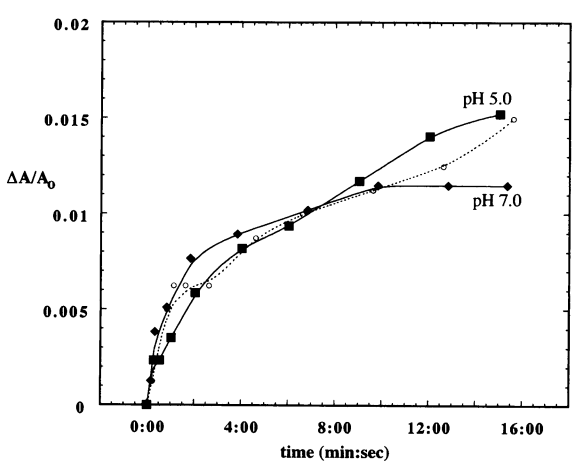

FIGURE 4 $\Delta A/A_o$ versus time for vesicles exposed to 10 μM of a nonhemolytic, fusion-defective mutant of wt-20 lacking the N-terminal glycine: ■, pH 5.0; ◆, pH 7.0. These plots are very similar to the DMSO plots in Fig. 2 *B*, in which no peptide was present. Repeated here is a plot for the apparent area expansion of a vesicle exposed to 1% DMSO at a pH of 5.0 (○), corresponding to the amount of DMSO used in these experiments. The apparent increase in $\Delta A/A_o$ is simply due to a slight difference in osmotic strength between the two chambers and a small amount of evaporation that occurs over long time scales, which leads to an increase in the vesicle projection.

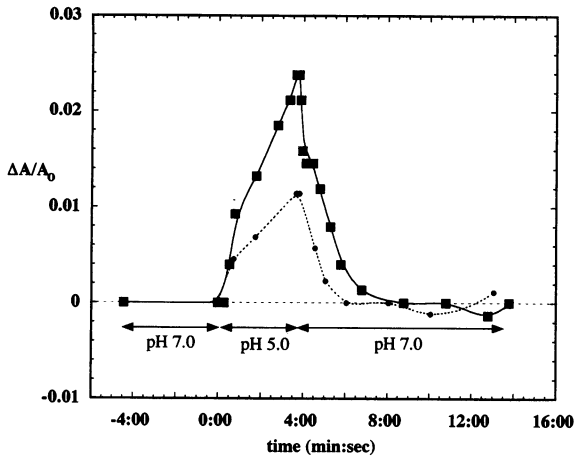

FIGURE 5 Effect of pH change for a vesicle exposed to wt-20 (■). Vesicle exposed to 2.5 μM wt-20, pH 7.0, was transferred to a 2.5 μM wt-20 solution at pH 5.0. Transfer resulted in an increase in $\Delta A/A_0$ due to the insertion of wt-20 into the lipid bilayer. Placing the vesicle in a pH 7.0 solution results in complete recovery of the original surface area and normal mechanical properties. As a control, the experiment was repeated without wt-20 (●) to obtain the apparent change in $\Delta A/A_0$ resulting from osmotic strength differences between the two chamber sections.

the lysis tension was within normal range, 7.48 dyn/cm, after 15 min of exposure.

Effect of concentration change on insertion

Reversibility of wt-20 peptide uptake was tested by transferring a vesicle with inserted wt-20 in a pH 5.0, 5 μM, wt-20 solution to a solution free of the peptide at a pH of 5.0

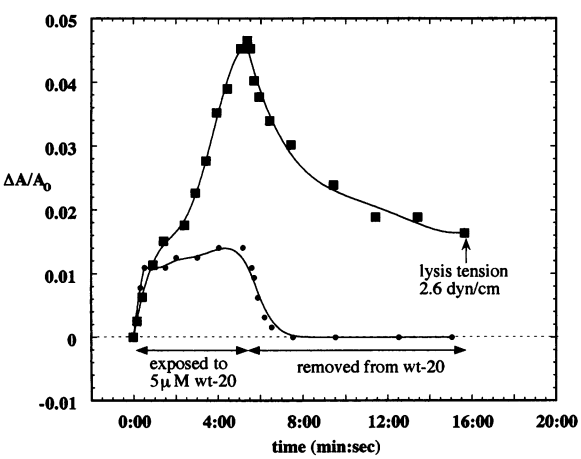

FIGURE 6 Exposure of a vesicle to a 5 μM wt-20 solution at a pH of 5.0 (■) and transfer to a solution at the same pH containing no wt-20 resulted in nearly complete desorption of wt-20. After partial desorption, the vesicle has a lowered lysis tension (2.6 dyn/cm in comparison to a mean lysis tension of 7.0 for test vesicles), probably as a result of perturbation of the membrane bilayer by the presence of wt-20 in the bilayer. As a control, the experiment was repeated without wt-20 (●) to obtain the apparent change in $\Delta A/A_0$ resulting from osmotic strength differences between the two chambers.

(Fig. 6). This transfer resulted in partial recovery of the initial area of the vesicle. One-half of the area expansion remained, presumably from membrane-bound peptide. A lysis tension test found the vesicle to be weakened (2.3 dyn/cm) in comparison with the range of lysis tensions for control vesicles reported above. However, the area compressibility of the vesicle (167 dyn/cm) was within normal range, indicating that a decrease in area compressibility was not responsible for the lowered lysis tension. Therefore, defects formed in the vesicle membrane were most likely responsible for the lowered lysis tension.

Effect of concentration on insertion

To determine the effect of bulk concentration on the adsorption of wt-20, we exposed vesicles to wt-20 at several concentrations (Table 1 and Fig. 7). Exposure of a vesicle to 1 μM wt-20 at pH 4.5 resulted in an increase in projection length indistinguishable from controls containing DMSO at pH 5.0 (Figs. 4 and 7). Exposure to 5 μM wt-20 resulted in an average $\Delta A/A_{0,\,max}$ of ~0.10. For the plot shown (Fig. 7, 5 μM wt-20), we observed a slower rate of change of $\Delta A/A_0$ followed by a more rapid $\Delta A/A_0$ change with time and the formation of defects. We saw similar changes in $\{\Delta A/A_0\}/t$ when a vesicle became permeable to glucose early in the adsorption (data not shown). Apparently, the porous defects in the membrane can seal, leading to an increased area expansion rate. At 20 μM wt-20, the entire area expansion and volume expansion cycle occurs in a matter of 20 s. The $\Delta A/A_{0,max}$ obtained before permeation was ~0.12.

DISCUSSION

A major finding of this work is the rapid area expansion of the lipid membrane of vesicles (99% SOPC) exposed to bulk fusion peptide concentrations near 10 μM. The observed extent of area expansion and subsequent permeation

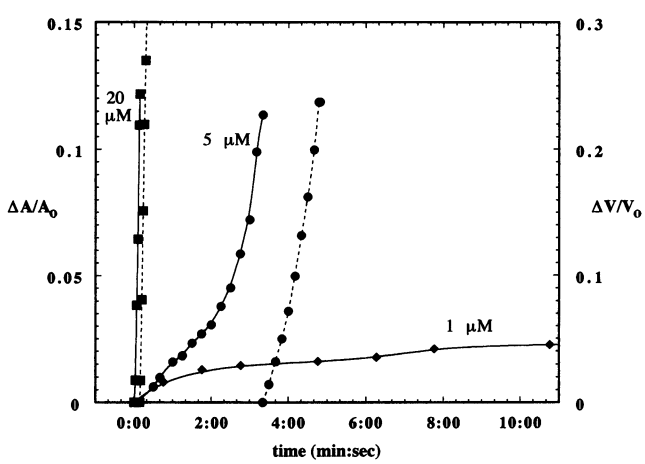

FIGURE 7 ——, $\Delta A/A_0$ versus time; and – – –, $\Delta V/V_0$ versus time for vesicles exposed to different concentrations of wt-20 at a pH of 4.5: ◆, 1 μM; ●, 5 μM; ■, 20 μM.

to glucose are pH dependent. The pH dependence of the extent and rate of area expansion and vesicle permeation corresponds closely to increases in fusogenic and hemolytic activity of this peptide when the pH is lowered to ~5 (Wharton et al., 1988). These observations suggest that the ability of a peptide to induce area expansion (through insertion) is an important determinant of fusogenic and lytic activity. Our results show that the native hemagglutinin fusion peptide (wt-20) from the X31 strain of influenza virus is taken up rapidly into SOPC:POPS (99:1) membranes, resulting in large increases in membrane surface area (as much as 11% of the original area). In a pH range from 4.5 to 7.0, exposure to 10 μM wt-20 resulted in the permeation of the vesicles to glucose (diameter $\approx$ 0.5 nm), leading to vesicle swelling and rupture. Exposure of vesicles to wt-20 at pH 5 resulted in approximately three times greater $\Delta A/A_{o,max}$ in comparison to pH 7 at the same bulk concentration. In general, the extent of area expansion appears to be closely related to the time required for the membrane to become porous (Table 1).

Insertion of the wt-20 peptide can be triggered simply by lowering the pH from neutral pH to pH 5.0. wt-20 peptide insertion is mainly reversible at pH 5.0 and can be completely reversed if the pH is returned to neutrality at micromolar concentrations. In contrast, Morris et al. (1989) observed that when fusion was mediated by the entire hemagglutinin protein, the process could only be reversed by raising the pH in the first 2–10 s. However, fusion involves major rearrangements of the lipid bilayer structure that are probably not involved here.

An estimate of the number of wt-20 peptides inserted into the membrane can be obtained by using the volume occupied by each residue (Gallaher et al., 1992). Assuming that the wt-20 peptide is inserted transmembrane, with a bilayer thickness of 40 Å (Marsh, 1990), the peptide will occupy an area of ~30 Å^2 (this estimate is probably a lower bound on the surface area; Burger et al., 1991, report that the minimum "monolayer" surface area is 290 Å^2 per HA fusion peptide). For a value $\Delta A/A_o$ of ~0.1, there will be ~6×10^8 wt-20 peptides inserted in the bilayer. This is in comparison to ~6×10^9 SOPC molecules in the bilayer of the vesicle. With the concentration of peptide utilized (10 μM), the amount of peptide depleted from the surrounding solution would occupy a shell volume ~20 μm thick around the vesicle. Utilizing the Stokes-Einstein relation to estimate diffusion coefficient of a wt-20 peptide of radius 10 Å and an outer bound on the depletion layer of 20 μm thick around the vesicle, the flux of peptide to the bilayer surface (~6×10^{12} molecules/(cm^2 s)) is more than 10% of the range of insertion rates observed here for 10 μM wt-20 at pH 5. The actual depletion layer would probably be much less than 20 μm—particularly when the vesicle is initially exposed to wt-20 and very little peptide has inserted into the bilayer. Because the flux can be approximated as being inversely proportional to the depletion layer thickness, a smaller depletion layer will yield a higher flux. These estimations indicate that the faster insertion rates observed here (e.g., for 10 μM pH 5 wt-20) may be diffusion limited. If the peptide is inserted only in the outer bilayer and the inner bilayer is stretched, the amount of peptide inserted can be estimated at ~3×10^8 wt-20 for a $\Delta A/A_o$ of ~0.1.

An important finding of the present study is the complete lack of area expansion of the bilayer in the presence of a mutant of wt-20 in which the N-terminal glycine is absent. This ΔG1 peptide shows an area expansion plot at both pH 5.0 and pH 7.0 similar to those of peptide-absent controls. This result corresponds with the inability of this peptide to hemolyse red blood cells, shown by Wharton et al. (1988), and the lack of fusion activity of cells expressing HA with cleaved N-terminal glycine (Steinhauer et al., 1995). Our results with ΔG1 suggest that this peptide does not embed in the membrane bilayer. We reach this conclusion because of the lack of area expansion that occurs when this peptide is introduced to the bilayer in comparison to the wt-20 peptide and other amphiphiles that insert into the bilayer previously studied by micropipette aspiration (Simon et al., 1994; Needham and Zhelev, 1995). In contrast to the work presented here, tryptophan fluorescence studies by Wharton et al. (1988) and Gray et al. (1996) showed that a significant blue shift occurred when ΔG1 was placed with phosphatidylcholine vesicles at pH 7 and even more pronounced at pH 5, indicating that the tryptophans were sampling a hydrophobic environment. It is possible that the experimental conditions were different enough in our experiments to preclude the association of ΔG1 with lipid membranes. A particularly significant difference is the use of small unilamellar vesicles in previous tryptophan fluorescence studies (Gray et al., 1996; Wharton et al., 1988) and the use of much larger (20–30 μm) low tension (below the stretching dominated regime; Evans and Rawicz, 1990), minimal curvature vesicles used in this study. It is possible that the larger, stress-free vesicles used in this study more closely resemble the cell membrane. Thus, like the hemolytic studies, we do not see any perturbation of the membrane with the use of ΔG1. It is also possible that ΔG1 can adsorb to the membrane, but does not intercalate. In support of this possibility, Gray et al. (1996) have shown that ΔG1 interacts more strongly with lipid headgroups in comparison to the wild-type peptide. However, we have been unsuccessful in using preexposure of vesicles to ΔG1 peptide as a means of blocking wt-20 binding (data not shown).

In the case of wt-20, we do see a large change in the area expansion rate and maximum area expansion as the pH is lowered, and this is in agreement with the tryptophan fluorescence data of Wharton et al. (1988). In their work, there was a more significant blue shift of the tryptophan fluorescence for wt-20 in the presence of vesicles of phosphatidylcholine at a pH of 5 in comparison to a pH of 7.

In similar work studying the adsorption of lysophosphatidylcholine (lysoPC) into the bilayer, using micropipette aspiration, it was shown that lysoPC adsorbs and intercalates rapidly into the outer monolayer, with a slower rate of flip-flop to the inner monolayer of the bilayer (Needham and Zhelev, 1995). If this were the case here, the area

expansion observed would be almost entirely the result of an increased mass of the outer monolayer. If the wt-20 peptides adsorb much more rapidly to the outer monolayer, then redistribution (flip-flop) processes occur, bending stresses will certainly be significant, as a bilayer can only be stretched by ~5% before mechanical failure occurs (Evans and Needham, 1987). Bending stress of the outer monolayer may be relieved by the formation of nanometer-scale pores and the rapid flip-flop of phospholipid or peptide from the outer monolayer to the inner monolayer (Fattal et al., 1994). This interpretation of the mechanism of wt-20 fusion peptide membrane disruption at low pH is supported by our data, showing that when exposure to the fusion peptide wt-20 resulted in less than ~5% area expansion, we observe an area expansion plateau and transient membrane stability (pH 7.0 and pH 6.0).

An intriguing question is: Why does the membrane become porous (at long times), even when the amount of area expansion is small and has leveled off? It is possible that a combination of factors may be required for the formation of porous defects when the membrane area has expanded slowly. Possibly, a quantity of the active conformation of the peptide must be present (the peptide may settle into a more active form with time), or a period of time may be required for a peptide to aggregate (self-associate) in the membrane, causing local perturbations. Another interesting question is: Why can the membrane area be expanded by as much as 11% and why does that appear to be the maximum area expansion possible. Perhaps, for short periods of time, the membrane can be expanded more than the critical 5% in which a bilayer fails. It may take time for the membrane to become porous and for flip-flop processes to occur. We may also ask: Do the densities of peptides inserted into the bilayers here compare with the densities of hemagglutinin spike proteins on a virion surface? The intact virion surface is covered with approximately one hemagglutinin protein per 80 nm^2 (Burger et al., 1991). Therefore, presumably, the virion could insert approximately three HA fusion peptides into the target membrane per 80 nm^2 over a small area of contact (each HA protein contains three fusion peptides). The largest vesicle area expansion measured here would correspond to an unrealistically high HA fusion peptide coverage of one peptide per 3 nm^2 (assuming 30 $Å^2$/wt-20 as a lower bound). However, area expansions of $\Delta A/A_o$ = 0.01 (pH 7, 10 μM wt-20) compare more closely to the virion surface coverage. Even at these low area coverages, porous defects are formed, although over a longer time.

Our observations here help explain our earlier work (Soltesz and Hammer, 1995) and that of Wharton et al. (1988), Düzgüneş and Shavnin (1992), Düzgüneş and Gambale (1988), and Rafalski et al. (1991), who observed that exposure of vesicles or cells to micromolar amounts of wild-type hemagglutinin fusion peptides at low pH resulted in leakage of contents. Above all, it has been shown that the interaction of fusion peptides with a vesicle membrane is a dynamic process; the concentration and barrier properties of a membrane bilayer can be changed in seconds by exposure to the hemagglutinin fusion peptide of influenza virus. These results also suggest that kinetic studies of properties such as peptide conformation and lipid-peptide interaction may be as critical to discerning the complete mechanism of lipid disruption as studies in which measurements are taken at much larger time scales than the area expansion processes seen in these experiments.

We offer special thanks to the members of Dr. Richard Waugh's laboratory, University of Rochester, New York, for their helpful guidance and expert advice regarding the micropipette aspiration technique.

The National Institutes of Health are acknowledged for support of this research (HL18208). MLL is grateful for the support of National Institutes of Health NRSA Postdoctoral Fellowship GM 16506-02. The ABI 431A peptide synthesizer was acquired with the help of a National Institutes of Health small equipment grant (GM 50483 to AJW). A. Waring was supported by NIH grant GM08140.

REFERENCES

Anderson, W. F. 1995. Gene therapy. *Sci. Am.* 273:124–127.

Angelova, M. I., S. Soleau, Ph. Méléard, J. F. Faucon, and P. Bothorel. 1992. Preparation of giant vesicles by external AC electric fields. Kinetics and applications. *Prog. Colloid Polym. Sci.* 89:127–131.

Bagai, S., A. Puri, R. Blumenthal, and D. P. Sarkar. 1993. Hemagglutinin-neuraminidase enhances F protein-mediated membrane fusion of reconstituted sendai virus envelopes with cells. *J. Virol.* 67:3312–3318.

Burger, K. N. J., S. A. Wharton, R. A. Demel, and A. J. Verkleij. 1991. The interaction of synthetic analogs of the N-terminal fusion sequence of influenza virus with a lipid monolayer. Comparison of fusion-active and fusion-defective analogs. *Biochim. Biophys. Acta.* 1065:121–129.

Clague, M. J., J. R. Knutson, R. Blumenthal, and A. Herrmann. 1991. Interaction of influenza hemagglutinin amino-terminal peptide with phospholipid vesicles: a fluorescence study. *Biochemistry.* 30: 5491–5497.

Curiel, D. T., S. Agarwal, E. Wagner, and M. Cotten. 1991. Adenovirus enhancement of transferin-polylysine-mediated gene delivery. *Proc. Natl. Acad. Sci. USA.* 88:8850–8854.

Cussler, E. L. 1984. Diffusion, Mass Transfer in Fluid Systems. Cambridge University Press, Cambridge.

Daniels, R. S., J. C. Downie, A. J. Hay, M. Knossow, J. J. Skehel, M. L. Wang, and D. C. Wiley. 1985. Fusion mutants of the influenza virus hemagglutinin glycoprotein. *Cell.* 40:431–439.

Düzgünes, N., and F. Gambale. 1988. Membrane action of synthetic N-terminal peptides of influenza virus hemagglutinin and its mutants. *FEBS Lett.* 227:110–114.

Düzgünes, N., and S. A. Shavnin. 1992. Membrane destabilization by N-terminal peptides of viral envelope proteins. *J. Membr. Biol.* 128: 71–80.

Evans, E., and D. Needham. 1987. Physical properties of surfactant bilayer membranes: thermal transitions, elasticity, rigidity, cohesion, and colloidal interactions. *J. Phys. Chem.* 91:4219–4228.

Evans, E., and W. Rawicz. 1990. Entropy-driven tension and bending elasticity in condensed-fluid membranes. *Phys. Rev. Lett.* 64: 2094–2097.

Fattal, E., S. Nir, R. A. Parente, and F. C. Szoka, Jr. 1994. Pore-forming peptides induce rapid phospholipid flip-flop in membranes. *Biochemistry.* 33:6721–6731.

Fields, C. G., D. H. Lloyd, R. L. Macdonald, K. M. Ottenson, and R. L. Noble. 1991. HBTU activation for automated Fmoc solid-phase peptide synthesis. *Pept. Res.* 4:95–101.

Fonteijn, T. A. A., J. B. F. N. Engberts, S. Nir, and D. Hoekstra. 1992. Asymmetric fusion between synthetic di-*n*-dodecylphophate vesicles and virus membranes. *Biochim. Biophys. Acta.* 1110:185–192.

Gallaher, W. R., J. P. Segrest, and E. Hunter. 1992. Are fusion peptides really "sided" insertional helices? *Cell.* 70:531–532.

Gething, M. J., R. W. Doms, D. York, and J. White. 1986. Studies of the mechanism of membrane fusion: site-specific mutagenisis of the hemagglutinin of influenza virus. *J. Cell. Biol.* 102:11–23.

Glushakova, S. E., V. G. Omelyaneko, I. S. Lukashevitch, A. A. Bogdanov, Jr., A. B. Moshnikova, A. T. Kozytch, and V. P. Torchilin. 1992. The fusion of artificial lipid membranes induced by the synthetic arenavirus "fusion peptide." *Biochim. Biophys. Acta.* 1110:202–208.

Gray, C., S. A. Tatullian, S. A. Wharton, and L. K. Tamm. 1996. Effect of the N-terminal glycine on the secondary structure, orientation, and interaction of the influenza hemagglutinin fusion peptide with lipid bilayers. *Biophys. J.* 70:2275–2286.

Grewe, C., A. Beck, and H. R. Gelderblom. 1990. HIV: early virus-cell interactions. *J. AIDS.* 3:965–974.

Harter, C., P. James, T. Bächi, G. Semenza, and J. Brunner. 1989. Hydrophobic binding of the ectodomain of influenza hemagglutinin to membranes occurs through the "fusion peptide." *J. Biol. Chem.* 264: 6459–6464.

Helenius, A., J. Kartenbeck, K. Simons, and E. Fries. 1980. On the entry of Semiliki forest virus into BHK-21 cells. *J. Cell Biol.* 84:404–420.

Hoekstra, D. 1990. Membrane fusion of enveloped viruses: Especially a matter of proteins. *J. Bioenerg. Biomembr.* 22:121–155.

Hoekstra, D., K. Klappe, T. deBoer, and J. Wilschut. 1985. Characterization of the fusogenic properties of sendai virus: kinetics of fusion with erythrocyte membranes. *Biochemistry.* 24:4739–4745.

Hug, P., and R. G. Sleight. 1994. Fusogenic virosomes prepared by partitioning of vesicular stomatitis virus G protein into preformed vesicles. *J. Biol. Chem.* 269:4050–4056.

Ishiguro, R., N. Kimura, and S. Takahashi. 1993. Orientation of fusion-active synthetic peptides in phospholipid bilayers: determination by Fourier transform infrared spectroscopy. *Biochemistry.* 32:9792–9797.

Lear, J. D., and W. F. DeGrado. 1987. Membrane binding and conformational properties of peptides representing the NH_2 terminus of influenza HA-2. *J. Biol. Chem.* 262:6500–6505.

Marsh, D. 1990. CRC Handbook of Lipid Bilayers. CRC Press, Boca Raton, FL.

Matlin, K. S., H. Reggio, A. Helenius, and K. Simons. 1981. Infectious entry pathway of influenza virus in a canine kidney cell line. *J. Cell Biol.* 91:601–613.

McClure, M. O., M. Marsh, and R. A. Weiss. 1988. Human immunodeficiency virus infection of CD4-bearing cells occurs by a pH-independent mechanism. *EMBO J.* 7:513–518.

Melikyan, G. B., W. D. Niles, M. E. Peeples, and F. S. Cohen. 1993. Influenza hemagglutinin-mediated fusion pores connecting cells to planar membranes: flickering to final expansion. *J. Gen. Phys.* 102: 1131–1149.

Mobley, P. W., H. F. Lee, C. C. Curtain, A. Kirkpatrick, A. J. Waring, and L. M. Gordon. 1995. The amino-terminal peptide of HIV-1 glycoprotein 41 fuses human erythrocytes. *Biochim. Biophys. Acta.* 1271:304–314.

Morris, S. J., D. P. Sarkar, J. M. White, and R. Blumenthal. 1989. Kinetics of pH-dependent fusion between 3T3 fibroblasts expressing influenza hemagglutinin and red blood cells. *J. Biol. Chem.* 264:3972–3978.

Morsy, M. A., K. Mitani, P. Clemens, and C. T. Caskey. 1993. Progress toward human gene therapy. *JAMA.* 270:2338–2345.

Needham, D. 1993. Measurement of interbilayer adhesion energies. *Methods Enzymol.* 220:111–130.

Needham, D., and D. V. Zhelev. 1995. Lysolipid exchange with lipid vesicle membranes. *Ann. Biomed. Eng.* 23:287–298.

Plank, C., B. Oberhauser, K. Mechtler, C. Koch, and E. Wagner. 1994. The influence of endosome-disruptive peptides on gene transfer using synthetic virus-like gene transfer systems. *J. Biol. Chem.* 269: 12918–12924.

Rafalski, M., A. Ortiz, A. Rockwell, L. C. van Ginkel, J. D. Lear, W. F. DeGrado, and J. Wilschut. 1991. Membrane fusion activity of the influenza virus hemagglutinin: interaction of HA2 N-terminal peptides with phospholipid vesicles. *Biochemistry.* 30:10211–10220.

Simon, S. A., E. A. Disalvo, K. Gawrisch, V. Borovyagin, E. Toone, S. S. Schiffman, D. Needham, and T. J. McIntosh. 1994. Increased adhesion between neutral lipid bilayers: interbilayer bridges formed by tannic acid. *Biophys. J.* 66:1943–1958.

Sinangil, F., A. Loyter, and D. J. Volsky. 1988. Quantitative measurement of fusion between human immunodeficiency virus and cultured cells using membrane fluorescence dequenching. *FEBS Lett.* 239:88–92.

Slepushkin, V. A., G. B. Melikyan, M. S. Sidorova, V. M. Chumakov, S. M. Andreev, R. A. Manulyan, and E. V. Karamov. 1990. Interaction of human immunodeficiency virus (HIV-1) fusion peptides with artificial lipid membranes. *Biochem. Biophys. Res. Commun.* 172:952–957.

Soltesz, S. A., and D. A. Hammer. 1995. Micropipette manipulation techniques for the monitoring of pH-dependent membrane lysis as induced by the fusion peptide of influenza virus. *Biophys. J.* 68: 315–225.

Stegmann, T., J. M. Delfino, F. M. Richards, and A. Helenius. 1991. The HA2 subunit of influenza hemagglutinin inserts into the target membrane prior to fusion. *J. Biol. Chem.* 266:18404–18410.

Stegmann, T., D. Hoekstra, G. Scherphof, and J. Wischut. 1985. Kinetics of pH-dependent fusion between influenza virus and liposomes. *Biochemistry.* 24:3107–3113.

Steinhauer, D. A., S. A. Wharton, J. J. Skehel, and D. C. Wiley. 1995. Studies of the membrane fusion activities of fusion peptide mutants or influenza virus hemagglutinin. *J. Virol.* 69:6643–6651.

Struck, D. K., D. Hoekstra, and R. E. Pagano. 1981. Use of resonance energy transfer to monitor membrane fusion. *Biochemistry.* 20: 4093–4099.

Wagner, E., C. Plank, K. Zatloukal, M. Cotten, and M. L. Birnstiel. 1992. Influenza virus hemagglutinin HA-2 N-terminal fusogenic peptides augment gene transfer by transferrin-polylysine-DNA complexes: toward a synthetic virus-like gene-transfer vehicle. *Proc. Natl. Acad. Sci. USA.* 89:7934–7938.

Weber, T., G. Paesold, C. Galli, R. Mischler, G. Semenza, and J. Brunner. 1994. Evidence for H^+-induced insertion of influenza hemagglutinin HA2 N-terminal segment into viral membrane. *J. Biol. Chem.* 269: 18353–18358.

Wharton, S. A., S. R. Martin, R. W. H. Ruigrok, J. J. Skehel, and D. C. Wiley. 1988. Membrane fusion by peptide analogues of influenza virus haemagglutinin. *J. Gen. Virol.* 69:1847–1857.

White, J. M. 1990. Viral and cellular membrane fusion proteins. *Annu. Rev. Physiol.* 52:675–697.

White, J. M. 1992. Membrane fusion. *Science.* 258:917–924.

Zhelev, D. V., and D. Needham. 1993. Tension-stabilized pores in giant vesicles: determination of pore size and pore line tension. *Biochim. Biophys. Acta.* 1147:89–104.

Zimmerberg, J., R. Blumenthal, D. P. Sarkar, M. Curran, and S. J. Morris. 1994. Restricted movement of lipid and aqueous dyes through pores formed by influenza hemagglutinin during cell fusion. *J. Cell Biol.* 127:1885–1894.